LIQUID CRYSTALS, 1998, VOL. 24, NO. 1, 117–125

Topological defects in dispersed liquid crystals, or words and worlds around liquid crystal drops

by O. D. LAVRENTOVICH

Chemical Physics Interdisciplinary Program and Liquid Crystal Institute,
Kent State University, Kent, Ohio 44242, USA

Presented at the Capri Symposium in Honour of George W. Gray, FRS held at the Hotel Palatium, Capri, 11–14 September 1996

The structure of dispersed liquid crystal droplets is controlled by a balance of the bulk elasticity, surface tension, and surface anchoring. For sufficiently large droplets with radius $R > K/W_a$, where K is the bulk elastic constant and W_a is the anchoring coefficient, the surface terms prevail. As a result, the equilibrium states of large droplets contain topologically stable defects. Application of topological theorems to defect structures, e.g. monopoles, boojums and hedgehogs is reviewed.

1. Introduction

Thermotropic liquid crystals and dispersed-phase systems are two fields of active research in soft matter science usually considered as independent. Recent years have shown a growing interest in dispersions of liquid crystals where the dispersed phase is a thermotropic liquid crystal.

Apparently, the first liquid crystalline dispersions were prepared in the 1890s by Otto Lehmann [1] who mixed *para*-azoxyanisole with different fluids such as Canadian balsam, colophony, mineral oil, etc. The aim was nothing other than to decipher the nature of the liquid crystalline order. Observations with a polarizing microscope revealed floating spherical droplets with beautiful birefringent textures. Lehmann recognized that the birefringence was caused by an ordered alignment of elongated 'elementary units' (molecules) inside the droplets. In the simplest model, the molecules were supposed to orient along the meridians at the droplet surface. Thus the substance under study was really a 'liquid crystal': it formed spherical droplets like a fluid and at the same time possessed an ordered structure like crystals.

Lehmann's ordered droplets were practically forgotten as soon as it became clear that liquid crystals did really exist as distinctive phases. Even in the 1930–1970s, when Oparin and his followers developed ideas of the coacervate origin of life [2] and when biochemists studied practically all the possible variations of dispersions to create 'protocells', liquid crystal droplets as plausible 'protocells' attracted little attention. Nevertheless, observations that some coacervate droplets are optically anisotropic have been reported [3].

It was not until the last decade that there came a true revival of interest in liquid crystalline droplets. The invention of polymer dispersed liquid crystals (PDLCs) as a medium for electro-optical devices [4, 5] was a spectacular manifestation of the unique properties of anisotropic dispersions. Two basic features, i.e. (1) the ordered inner structure of the dispersed particles and (2) the small scale of confinement in which bulk and surface interactions are in direct competition, make liquid crystalline dispersions distinctive and more complex than their isotropic counterparts or continuous liquid crystalline media.

The equilibrium states of liquid crystal dispersions often contain topologically stable defects. Some of them are rather unusual, as, for example, monopoles in cholesteric and smectic C droplets which are analogues of the Dirac monopole, a hypothetical elementary magnetic charge. The aim of this short review is to present basic structural and topological properties of liquid crystal droplets and to recall some stimulating parallels with other fields of physics.

2. Basic properties of liquid crystal droplets

The equilibrium state of liquid crystal droplets, and similar objects such as isotropic droplets or monodomain solid crystals bounded by an isotropic medium, is defined by the minimum of the free energy functional that can be formally decomposed into a volume and a surface part:

$$F = F_V + F_S = \int_V f \, dV + \int_S \sigma \, dS. \qquad (1)$$

Here V is the droplet's volume, f the bulk free energy density, S the area of the bounding surface and σ the surface free energy per unit area.

0267–8292/98 $12·00

For isotropic droplets, σ is constant. If there is no exchange of molecules with the surrounding matrix (V is constant), the equilibrium shape is found by minimizing the surface energy. The droplet adopts a spherical shape of radius $R = (3V/4\pi)^{1/3}$. If the droplet nucleates during a first-order phase transition, f should be understood as the difference in free energy density between the surrounding matrix (vapour, metastable phase) and the stable nucleating phase. Then the free energy (1) is defined by the bulk term $F_v = \frac{4}{3}\pi f R^3 < 0$ and by the surface term $F_s = 4\pi\sigma R^2 > 0$. A spherical embryo larger than $R_c = 2\sigma/f$ grows indefinitely since the bulk energy gain $\sim R^3$ outweighs the surface energy penalty $\sim R^2$.

In solid crystals, the bulk energy of distortions that might be caused by the surface is prohibitively high and the variational problem for equation (1) is solved under the constraint that the crystal preserves its ideal lattice structure. The surface energy σ depends on crystallographic orientation. This dependence can contain 'cusps' at which the first derivative of σ is discontinuous. The cusps lead to a faceted shape of a crystal that can be reconstructed through the well-known Wulff procedure.

Liquid crystal droplets present the most difficult case of the minimization problem since, first, σ depends on the surface orientation of the molecules and, second, surface and bulk energies are often comparable. In nematics, the amplitude W_a of the angular dependent part of σ ('anchoring energy') is usually much smaller than the energy σ_0 needed to extend the area of the surface preserving the equilibrium director orientation. Typical values for the liquid crystalline cyanobiphenyls–glycerin pairs are $\sigma_0 \sim (10^{-3}\text{–}10^{-2})\ \mathrm{J\,m^{-2}}$ [6] and $W_a \sim (10^{-6}\text{–}10^{-5})\ \mathrm{J\,m^{-2}}$ [7]. Surfactants such as lecithin decrease σ_0 by an order of magnitude [7].

Representative estimates are $\sigma_0 R^2$ for the isotropic part of the surface energy, $W_a R^2$ for the anisotropic surface energy, and, finally, KR for F_v, where $K \sim 10^{-11}$ N is the bulk elastic constant. Note that the bulk elastic energy scales *linearly* with R rather than as R^3. Thus, in contrast to nucleating drops, the surface energies outweigh the bulk elastic energy for large R.

The first consequence of the estimates above is that realistic liquid crystal droplets are practically spherical: the length $l_\sigma = K/\sigma_0$ is usually of the order of a molecular length.

The second consequence is that for a given pair liquid crystal–isotropic fluid matrix, the structure of the droplets is greatly influenced by their size. Droplets with $R \ll K/W_a$ avoid spatial variations of the director $\mathbf{n}$ and set $\mathbf{n}(\mathbf{r}) = const$ at the expense of violated boundary conditions. In contrast, large droplets satisfy boundary conditions by aligning molecules along the easy direction(s). Since the boundary of the droplet is curved, this anchoring effect leads to the distorted director in the bulk, figure 1. For example, as shown by Williams [8] for tangentially anchored droplets with a Rapini–Papoular anchoring potential, the minimum of the total energy ($F_V + F_S$) at $R \to \infty$ is the same as the minimum of the Frank–Oseen energy F_V with the restriction that $\mathbf{n}$ is strictly tangential to the surface.

With typical $W_a \approx 10^{-5}\ \mathrm{J\,m^{-2}}$ and $K \approx 10^{-11}$ N, the characteristic anchoring length $l_W = K/W_a$ is of the order of 1 μm and normally much larger than l_σ. Droplets with $R \gg l_W$ are 'large' and contain defects in equilibrium. A similar balance of surface and bulk energies in smectic A droplets results in focal-conic defects of characteristic size $\rho > K/W_a$ that fit the boundary conditions and thus save surface energy $\sim\rho^2$ at the expense of the elastic energy $\sim\rho$ [9]; the difference is that W_a should be understood as the surface energy difference for normal and tangential orientation. As discussed in the next section, nematic droplets with $R \gg l_W$ can be described on the basis of elementary topological properties of the bounding surface.

3. Elements of topological description of defects

For $R \gg l_W$, the director of the interface makes an equilibrium polar angle α_0 with the surface normal $\mathbf{k}$. Even without solving the minimization problem, one can establish general and useful topological properties of structures that occur inside these droplets as long as α_0 is fixed. This possibility stems from two theorems of differential geometry, i.e. the Gauss and Poincaré theorems. The theorems connect the total topological charges of point defects in the vector field to the so-called Euler characteristics E of the bounding surface.

Topological charges play a key role in the classification of defects in condensed media as shown by Toulouse and Kléman [10] and Volovik and Mineev [11] on the basis of homotopy theory. The stability of the defect is guaranteed by the conservation of its topological charge. The laws of conservation of such charges, analogously to the laws of conservation of electric and other physical charges, regulate the decay and merging of defects, their creation, annihilation, and mutual transformation. The well-known example of the topological charge is the Frank

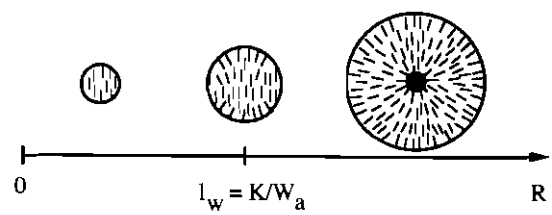

Figure 1. Schematic structures of nematic droplets with normal anchoring. Large droplets with $R \gg K/W_a$ contain topological defects in equilibrium; in small droplets with $R \ll K/W_a$ the director tends to be uniform.

index of a linear disclination. Similar characteristics can be introduced for point defects.

Analytically, the topological charge of a point defect in a t-dimensional vector field $(n_1, n_2, \ldots n_t)$, $\mathbf{n}^2 = 1$ is defined as an integral (e.g. ref. [12]):

$$N^{(t)} = \frac{1}{\Omega} \int_{S^{t-1}} \begin{vmatrix} n^1 & \ldots & \ldots & n^t \\ \dfrac{\partial n^1}{\partial u^1} & \ldots & \ldots & \dfrac{\partial n^t}{\partial u^1} \\ \ldots & \ldots & \ldots & \ldots \\ \dfrac{\partial n^1}{\partial u^{t-1}} & \ldots & \ldots & \dfrac{\partial n^t}{\partial u^{t-1}} \end{vmatrix} \mathrm{d}u^1 \ldots \mathrm{d}u^{t-1}, \tag{2}$$

where $u^1, \ldots u^{t-1}$ are coordinates specified on the sphere S^{t-1} surrounding the defect, and a normalizing coefficient Ω equals 4π for $t = 3$ and 2π for $t = 2$. For the case of $t = 2$, one has simply

$$N^{(2)} \equiv m = \frac{1}{2\pi} \oint \left(n^1 \frac{\mathrm{d}n^2}{\mathrm{d}l} - n^2 \frac{\mathrm{d}n^1}{\mathrm{d}l} \right) \mathrm{d}l = 0, \pm 1, \pm 2, \ldots, \tag{3}$$

where l is the natural parameter defined along the loop enclosing the defect point. For a bounded three-dimensional system, one can assign charges m to point defects in the surface vector field $\mathbf{t} = \mathbf{n} - \mathbf{k}(\mathbf{n} \cdot \mathbf{k})$ which is the projection of the director onto the surface. The number m shows how many times $\mathbf{t}$ rotates by the angle 2π when one moves once along a closed loop around the defect's centre.

For point defects in three-dimensional vector fields, equation (2) yields

$$N^{(3)} \equiv N = \frac{1}{4\pi} \iint \mathbf{n} \left[\frac{\partial \mathbf{n}}{\partial u} \times \frac{\partial \mathbf{n}}{\partial v} \right] \mathrm{d}u \, \mathrm{d}v. \tag{4}$$

If the vector field is parameterized as $\mathbf{n}(u, v) = \{\sin\theta \cos\varphi; \sin\theta \sin\varphi; \cos\theta\}$, with both the polar ($\theta$) and the azimuthal ($\varphi$) angles being functions of the coordinates u and v specified on a sphere S^2 surrounding the defect, then

$$N = \frac{1}{4\pi} \iint \left(\frac{\partial\theta}{\partial u} \frac{\partial\varphi}{\partial v} - \frac{\partial\theta}{\partial v} \frac{\partial\varphi}{\partial u} \right) \sin\theta \, \mathrm{d}u \, \mathrm{d}v. \tag{5}$$

For example, for a radial hedgehog $\mathbf{n} = \hat{\mathbf{r}}$ in spherical coordinates,

$$N = \frac{1}{4\pi} \iint \sin u \, \mathrm{d}u \, \mathrm{d}v = 1. \tag{6}$$

The number N shows how many times one meets all possible orientations of the vector field while moving around a closed surface surrounding the point defect. Note that in nematics, the sign of N is not defined: a substitution of $\mathbf{n}$ with $-\mathbf{n}$ obviously changes the sign of N in equation (4), but this substitution does not change the nematic state. In the absence of topological disclinations one might consider the director $\mathbf{n}$ as a vector.

The Euler characteristic E of the closed surface is a topological invariant that does not alter under smooth deformations. A practical way to calculate E is to draw a polygonal set at the surface and then calculate the number Vt of vertices, the number Ed of edges, and the number Fc of faces:

$$E = Vt - Ed + Fc. \tag{7}$$

As is easy to see, E does not depend on the particular choice of polygonal network; one always finds $E = 2$ for a sphere and $E = 0$ for a torus. The Euler characteristic can also be defined through the 'genus' g of the surface: $E = 2(1 - g)$. The genus g is the number of handles one has to attach to a sphere to transform it into the surface under consideration. Obviously, any spherical surface is assigned $g = 0$; a torus has $g = 1$; larger g's correspond to pretzels with g holes.

The Poincaré theorem states that the sum of all charges m of the vector field τ on the closed surface ($\alpha_0 \neq 0$) is equal to the Euler characteristic of the surface, e.g. 2 in the case of a sphere:

$$\sum_j m_j = E. \tag{8}$$

Figure 2 shows two possible defect configurations of a director field on a sphere.

The Gauss theorem states that if the vector field is normal to the closed surface, $\alpha_0 = 0$, then the sum of the topological charges N of all point defects inside the bounded volume is

$$\sum_i N_i = E/2, \tag{9}$$

i.e. 1 in the case of a sphere. A trivial illustration would be a radial hedgehog located in the centre of a sphere.

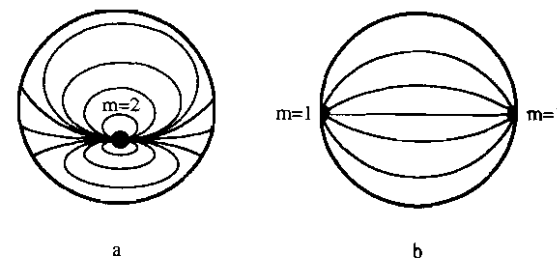

Figure 2. Possible configurations of the director field on a spherical surface with one $m = 2$ (*a*) or two $m = 1$ (*b*) point singularities; topological charges obey the Poincaré theorem (8).

4. Monopoles and boojums

The Dirac monopole [13], an elementary magnetic charge, is one of the most exciting illustrations of the topological theorems discussed above. Imagine a radial point defect in the magnetic field, $\mathbf{B} \| \mathbf{r}$, and draw imaginary concentric spheres around the centre of this 'hedgehog' so that the magnetic field is normal to these spheres. Obviously, the magnetic hedgehog has a topological charge $N = 1$. A vector-potential **A** that is normal to **B** is tangential to the imaginary spheres. Then in accordance with the Poincaré theorem, there must be at least one singularity in the vector-potential field on each sphere. These point singularities form a line, or Dirac string, emerging from the centre of the charge. Thus the Dirac monopole is a combination of a point defect-hedgehog $N = 1$ in the **B**-field with the attached semi-infinite 'disclination' $m = 2$ in the **A**-field.

Monopole defects similar to the Dirac monopole can occur in condensed matter. Soon after Osheroff, Richardson and Lee, see review [14], discovered the superfluid ^{3}He, Blaha [15] suggested that a monopole can be observed in 3He-A. Unlike ^{4}He which is composed of bosons, ^{3}He atoms are fermions and should pair to form a superfluid. However, in contrast to Cooper pairs in superconductors, the angular momentum of the atomic pair in ^{3}He is non-zero. The order parameter of the A phase is a triad of vectors ($\mathbf{l}, \Delta', \Delta''$), where **l** is the quantization axis of the orbital angular momentum of Cooper pairs; Δ' and Δ'' are perpendicular to **l**. In bounded volumes, **l** is always normal to the walls. Then in a spherical vessel one can hope to find a monopole: a radial point defect in the field **l** should be accompanied by disclinations in the Δ' and Δ'' fields (figures 2 and 3).

However, there is a way to reduce the energy of the system by moving the **l**-hedgehog towards the surface, so reducing the length of the linear disclinations (figure 3). The resulting surface singularity is simultaneously a hedgehog in the **l**-field and point defect with $m = 2$ in the Δ' and Δ'' fields. The possibility for line defects to shrink into a surface point singularity in ^{3}He-A was first recognized by Mermin [16]. Mermin called the point singularity 'boojum', inspired by Lewis Carroll's *The Hunting of the Snark*. In the poem, anyone encountering the imaginary creature 'boojum', softly and suddenly vanished away, just as disclinations do in the example above. The analogy is even deeper when one considers the superflow in ^{3}He-A. We refer the reader willing to learn more about boojums and their way into modern physics to Mermin's book [17] *Boojums All the Way Through*.

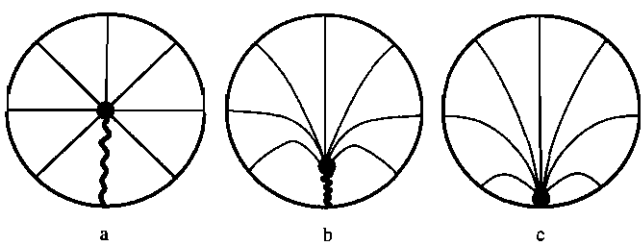

Figure 3. A monopole (*a*) and a boojum (*c*) in a spherical vessel filled with superfluid ^{3}He-A phase (cross-sections). The monopole is a combination of a point defect $N = 1$ in the vector field **l** (thin lines) that is normal to the boundary and a disclination line $m = 2$ (thick wavy line) in the vector fields Δ' and Δ'' tangential to the bounding surface. The monopole is unstable and transforms into the boojum (*c*): the disclination shrinks (*b*) into a point at the surface.

Mermin boojums can be observed in biaxial nematic liquid crystals where the order parameter is a triad of orthogonal directors. Let **n** be the director that characterizes both the uniaxial and the biaxial phases, and **l** the director that appears only in the biaxial phase; $\mathbf{l} \perp \mathbf{n}$. Suppose the matrix sets normal the orientation of **n** at the surface so that a point defect $N = 1$ exists somewhere in the bulk in accordance with the Gauss theorem. Director **l** that appears during the uniaxial–biaxial phase transition is tangential to the spherical surface and gives rise to a surface boojum that is simultaneously an $N = 1$ in **u** and an $m = 2$ defect in **l**.

Is there any mechanism in liquid crystals that might prevent a monopole from a decay into a boojum? Liquid crystals with layered structures such as cholesterics (Ch) and smectics C (SmC) offer such a stabilizing mechanism. Imagine, for example, a SmC droplet with concentric spherical packing of layers. The normal **n** to the layers forms a radial hedgehog. Since the molecules are tilted with respect to **n**, there is another vector field **t** of the projections of the long axes of the molecules. The field **t** is tangential to the SmC spherical layers and thus should contain disclinations (figure 2). In contrast to the biaxial nematic case, these lines are stable: any attempt to make them shorter violates the equidistance of the SmC layers [18, 19]. During the SmC–SmA phase transition, the disclination lines disappear since the vector field **t** disappears. Figure 4 illustrates both isolated radial point defects in SmA droplets and corresponding monopoles in SmC droplets. Similarly, in Ch droplets, the monopole might be stable if the pitch of the cholesteric is much shorter than the droplet radius. The monopole structure of cholesteric droplets has been observed by Robinson and explained by Frank and Price, see ref. [20].

5. Continuously defined topological characteristics

Topological charges such as Burgers vector of dislocation or the strength of a disclination are quantum. The quantum nature of these charges comes as a natural consequence of the fact that the order parameter has freedom to change without affecting the thermodynamic

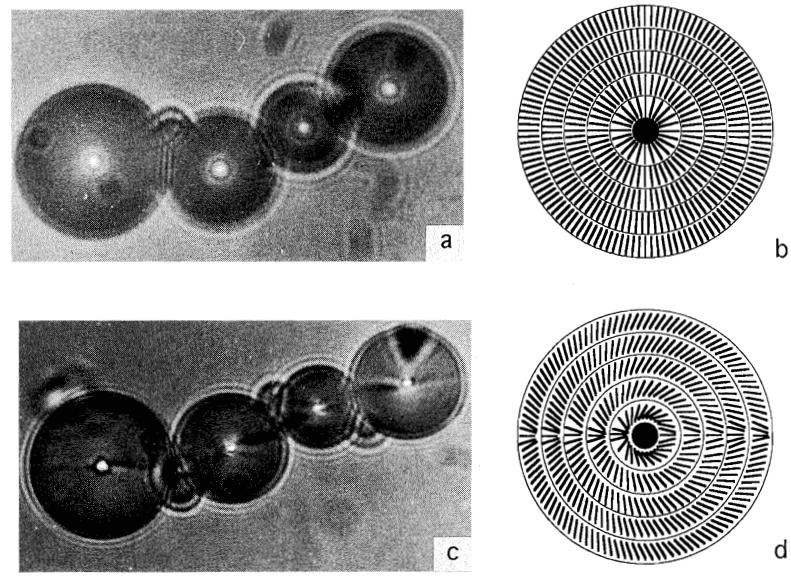

Figure 4. Spherical droplets of SmA (*a*) and SmC (*c*) liquid crystals suspended in a glycerin–lecithin matrix. The radius of the droplets in the microphotographs is about 15 μm. SmA droplets show hedgehog defects in the director field; the cores of the hedgehogs are located in the centres of the droplets. When the sample is cooled down and SmA transforms into SmC, these isolated point defects transform into monopoles: pairs of $m = 1$ appear in the field **t** that describes the tilt of the molecules within the smectic layers. Configuration of **t** at the spherical surface is illustrated by figure 2(*b*). Molecular schemes (*b*) and (*d*) show cross-sections of the SmA and SmC droplets, respectively.

potentials of the system [10, 11]. The manifold of corresponding states is called the order parameter space. For example, the director of a uniaxial nematic can take any orientation in space; all these orientations are energetically identical if the nematic rotates as a whole. The order parameter space is then a sphere S^2/Z_2 of a unit radius; any two antipodal points on this sphere are identical since the states **n** and $-\mathbf{n}$ are not distinguishable for the non-polar nematic phase. An example below illustrates how the concept of order parameter space leads to quantum topological charges.

The director field $\mathbf{n}(\mathbf{r})$ on any surface enclosing an elementary hedgehog $N = 1$ produces a mapping from the real space onto the order parameter space that completely covers the sphere S^2/Z_2. In other words, by going once around the hedgehog one meets all the possible orientations of **n**. To destroy the hedgehog, one has to make a hole in this cover, or, in other words, to melt the nematic in the real space along a line terminating at the defect core; the process requires energies much larger than the energy of the defect itself. A mapping of an $N = 2$ hedgehog spans the sphere two times, etc. There is no way to get a stable hedgehog with a non-integral charge: the corresponding cover of the sphere is incomplete and shrinks into a point which means that the director relaxes into a uniform state or a state with an integral charge.

Now consider a nematic droplet. Suppose there is a way to change continuously the boundary conditions on the surface of this droplet from, say, strictly tangential to strictly normal. Experimentally, it can be done by dispersing a nematic liquid crystal in a matrix composed of two components with opposite alignment tendencies and changing the temperature of the sample [21]. The droplet preserves the spherical shape since the anisotropic part of the nematic surface energy is smaller than the isotropic part, as already discussed. In the initial state with tangential anchoring, the droplet in equilibrium must contain two or one surface point defects—boojums with the total topological charge $m = 2$. In the final state, there should be no boojums (the director projection onto the surface vanishes), but the interior should contain a hedgehog with a charge $N = 1$. Under a smooth change in the surface angle α_0 from $\pi/2$ to 0, how do the boojums vanish and how does the hedgehog appear in their place? It is intuitively clear that the integer numbers m and N are not sufficient, and some continuously defined characteristics are needed to describe smooth transformations of the director field [21].

Consider the behaviour of an isolated boojum at a surface under changing boundary conditions (figure 5). At $\alpha_0 = \pi/2$, the boojum is characterized by the index $m = 1$ of the projection field $\mathbf{t} = \mathbf{n} - \mathbf{k}(\mathbf{n}\cdot\mathbf{k})$. In the interior, the boojum represents just one half of a hedgehog. If one surrounds the boojum by a hemisphere $\tilde{\gamma}$ with a unit radius, then the director marks all the points of this hemisphere. One can assign to the boojum a 'bulk' characteristic $A = 1/2$, since the area of the hemisphere is 1/2 of that of a sphere. When α_0 varies from $\pi/2$ to 0, the boojum either disappears [figure 5(*a*)–(*c*)], or transforms into a hedgehog [figure 5(*d*)–(*f*)]. Accordingly, A decreases to 0 or grows to 1. Quantitatively, A is defined as the integral (4) taken over the hemisphere $\tilde{\gamma}$:

$$A = \frac{1}{4\pi} \iint_{\tilde{\gamma}} \mathbf{n}\left[\frac{\partial \mathbf{n}}{\partial u} \times \frac{\partial \mathbf{n}}{\partial v}\right] du\, dv = \frac{m}{2}(\mathbf{n}\cdot\mathbf{k} - 1) + N. \tag{10}$$

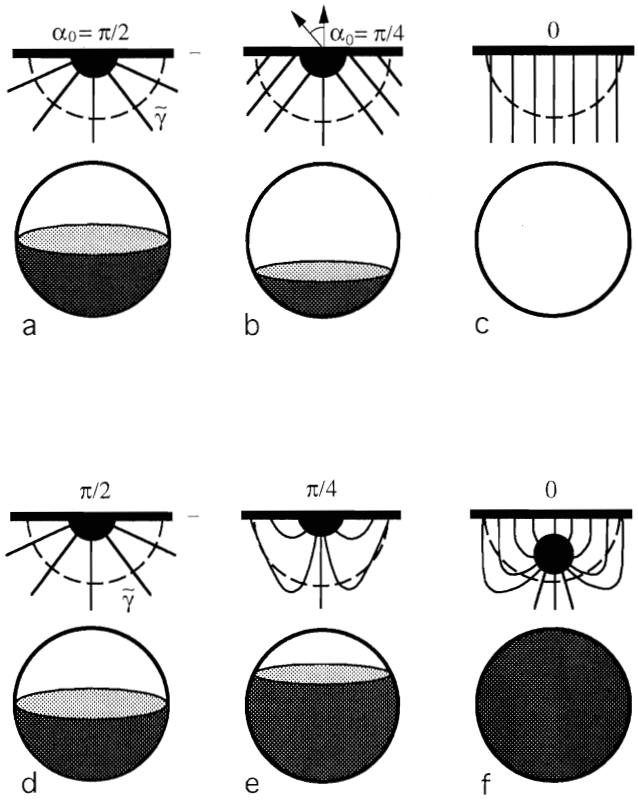

Figure 5. Two possible ways of boojum transformation under changing boundary conditions. The scenario (a, b, c) results in gradual disappearance of the defect, while the scenario (d, e, f) produces a point defect hedgehog. The corresponding characteristics A are shown as the shadowed areas on a sphere of the order parameter space below each boojum structure.

Here we treat **n** as a vector, rather than as a director, which is justified when there are no disclinations in the nematic bulk.

By using equation (10), one finds the topological 'bulk' charge N of the boojum since m is defined independently from the distribution of the projection field. For example, consider axisymmetric boojums with $m = 1$ located at the surface with a fixed angle α_0. The director field around a boojum can be parameterized in cylindrical coordinates as $n_r = \sin\theta(u, v)$, $\eta_\varphi = 0$, $\eta_z = \cos\theta(u, v)$, where θ is the angle between the vectors **k** and **n**. Then for these boojums,

$$A = \pm\frac{1}{2}\int \sin\theta\frac{\partial\theta}{\partial u}\,du = \pm\frac{1}{2}(\cos\alpha_0 \pm 1),$$

where the first pair of signs is defined by the sign of N and the second pair of signs is defined by the sign of $\partial\theta/\partial u$.

Consider the role of continuous A's in the behaviour of the drop as a whole. Assume that there are p point defects on its surface and q hedgehogs in its interior. Some of the hedgehogs can be stretched out into disclination rings; these rings, however, do not change the analysis since they are topologically equivalent to hedgehogs with integer charges $N = 0, \pm 1, \pm 2, \ldots$.

We surround all the defects in the bulk by a surface γ_1 and the entire surface of the droplet, together with the boojums, by a surface γ_2 (figure 6). The total topological charge of the hedgehogs enclosed by γ_1 is $\Sigma_i N_i$. The total charge enclosed by γ_2 is equal to the sum of the boojums' characteristics $\Sigma_j A_j$ and the characteristic of A_s of the droplet surface itself, which differs from zero because of the curvature of the surface. Taking the integral (5) over the drop surface with the boojums punched out, one finds $A_s = -\mathbf{n}\cdot\mathbf{k}$. Now, since there are no defects in between γ_1 and γ_2, the two total topological charges (taken with opposite signs) are equal to each other,

$$\sum_{b=1}^{p} A_b + A_s = -\sum_{a=p+1}^{p+q} N_a. \tag{11}$$

The last equation is the conservation law for topological charges in the closed droplet when the boundary conditions change. Some of the defects might vanish or appear, but the total charge is preserved by redistribution of A characteristics. It is easy to see that equation (11) gives conservation laws for both types of discretely defined charges. Really, for a bounding surface with the Euler characteristic E,

$$\sum_{b=1}^{p} A_b + A_s + \sum_{a=p+1}^{p+q} N_a = \frac{1}{2}\left(\sum_{b=1}^{p} m_b - E\right)(\mathbf{n}\cdot\mathbf{k} - 1) + \sum_{a=1}^{p+q} N_a - \frac{1}{2}E = 0; \tag{12}$$

therefore, $\Sigma_{b=1}^{p} m_b = E$ (for any $\alpha_0 \neq 0$) and $\sum_{a=1}^{p+q} N_a = E/2$ These equalities are nothing other than theorems (8) and (9).

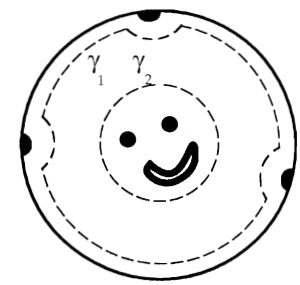

Figure 6. To find the conservation law for topological charges in the bounded volume, one uses two imaginary surfaces (dashed lines) to surround all the defects in the bulk and all the defects at the surface.

Relations above allow one to describe the 'topological dynamics' of defects in a nematic volume as redistribution of the continuous A characteristics under restrictions on the total charge and charges m, N. Different scenarios have been described in reference [21]. Basically, when the boundary conditions change and the characteristics of some defects change, other defects in the system should accordingly adjust their structure and topological characteristics to satisfy the conservation laws. Sometimes the process results in appearance of new defects or disappearance of the initial ones. For example, figure 7 illustrates the experimentally observed [21] scenario in which the decrease of the polar angle from $\alpha_0 = \pi/2$ [figure 7 (*a*)] to $\alpha_0 = 0$ [figure 7 (*e*)] results first in the appearance of the surface equatorial disclination [figure 7 (*b*)] and then in the disappearance of two boojums at the poles [figure 7 (*c*)]. After the boojums vanish away, the disclination ring shrinks into a point defect with $N = 1$ [figure 7 (*d*)] at the pole of the droplet. This state is topologically equivalent to a radial hedgehog. The equivalence is manifested by the last stage of the 'topological dynamics': the $N = 1$ defect relocates from the pole [figure 7 (*d*)] to the centre of the drop [figure 7 (*e*)].

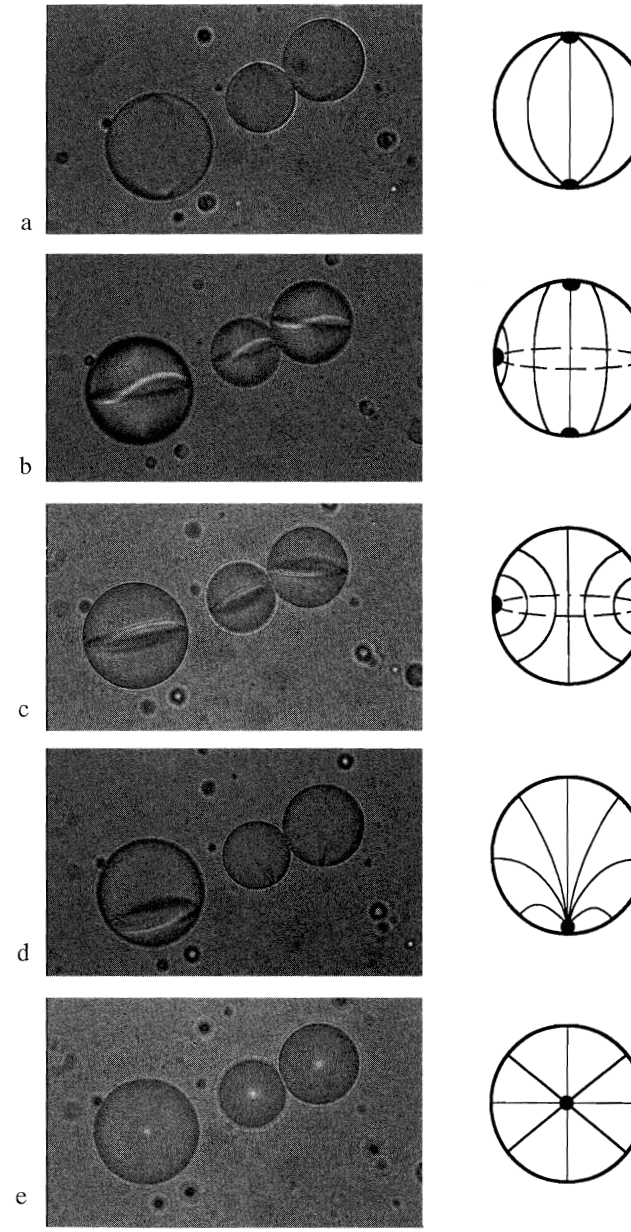

Figure 7. Topological dynamics of defects in nematic spherical droplets suspended in a glycerin–lecithin matrix. By changing the temperature of the sample, one changes the director orientation at the surface of the droplets from strictly tangential (*a*) to strictly normal (*e*). Defects transform to accommodate the changing boundary conditions but always preserve the total topological charge. The process includes formation of equatorial disclination line (*b*), gradual disappearance of boojums (*b*, *c*), shrinkage of the disclination into a surface point hedgehog (*d*) and, finally, relocation of the hedgehog from the surface into the bulk (*e*). The radius of the largest droplet in the microphotographs is about 20 μm. For more details, see the text and reference [21].

6. Phase ordering and stability of dispersions

Confinement and anchoring create topological defects in the equilibrium state of large ($R > K/W_a$) liquid crystal droplets. Non-trivial topology of the liquid crystal droplets might lead to a number of interesting physical consequences. One example is phase ordering in quenched systems, e.g. the transition from the isotropic melt into the nematic phase caused by rapid temperature decrease. The first-order isotropic–nematic transition occurs as nucleation of rounded nematic droplets floating in the isotropic sea. The conventional Kibble mechanism [22] treats the appearance of topological defects during the quenching as a result of coalescence of domains—droplets with different (but uniform within each domain) orientation of the director. This scenario is certainly relevant for the initial stage of the coalescence. However, as the droplets grow, the seed defects should show up as intrinsic singularities in *each* droplet that reached the size $\sim K/W_a$.

There is yet another aspect that makes the structural peculiarities of the droplets relevant to the problem of coalescence. As demonstrated experimentally by Terentjev [23], stability of nematic macroemulsions is greatly enhanced compared with that of their isotropic counterparts. The energy barrier for coalescence is defined mainly by the elastic constants of the liquid crystal and the surface tension (rather than by the anchoring energy). At the initial stage of coalescence,

the zone of contact of two droplets can be approximated by a disk of small radius $a \ll R$. The surface energy gain from the formation of such a contact area is $\sim\sigma_0 a^2$ (reduction in the total surface area of the two contacting droplets is $\sim a^2$), while the elastic penalty of additional distortions is at least of the order of $\sim Ka$. Figure 8 illustrates two contacting droplets with normal boundary conditions and a surface disclination ring of radius a and elastic energy $\sim Ka$. Appearance of the ring is dictated by topological reasons. The ring provides transition between the initial state with a pair of isolated hedgehogs and $N_1 + N_2 = 1 + 1 = 2$ and the final state with one hedgehog and $N = 1$. The contact area of two droplets would grow only if the elastic penalty $\sim Ka$ becomes smaller than the surface energy gain $\sim\sigma_0 a^2$, i.e. when $a > K/\sigma_0$. The energy barrier of coalescence is $\sim K^2/\sigma_0$. With $K \sim 10^{-11}$ N and low $\sigma_0 \sim 10^{-4}$ J m^{-2}, the energy barrier is high, $\sim 10^{-18}$ J, as compared with the thermal energy $\sim 4 \times 10^{-21}$ J at room temperature. Thus the nematic droplets are much more stable against coagulation compared with their isotropic counterparts with no bulk elasticity.

7. Conclusion

The phenomenon of surface anchoring leads to important consequences, e.g. equilibrium defect structures in liquid crystal dispersions. These defects are controlled by general topological laws and are similar to structures in other fields, such as magnetic monopoles or boojums in superfluids. The defects greatly influence not only individual, but also cooperative properties of droplets. Studies of these cooperative phenomena are currently being performed on emulsions in which isotropic droplets are surrounded by a nematic medium [24]. Here again the defects appear in the liquid crystalline matrix as a consequence of the anchoring phenomenon and topological constraints considered above. For example, for normal anchoring, each sufficiently large isotropic droplet or ball immersed in the liquid crystal matrix is topologically equivalent to a point hedgehog, and brings the topological charge $N = 1$ that must be compensated by a defect in the nematic matrix.

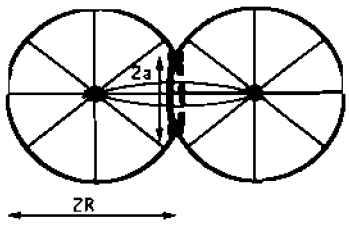

Figure 8. A scheme of two coalescing nematic droplets. An additional defect that forms in the system (surface disclination ring in the present case) hinders the coalescence (see the text).

During many years, liquid crystal structures have inspired hopes of gaining insight into the mechanisms of structural organization in biological systems (see the book by Needham [25] and the review by Gray [26]). A remarkable comparison of biological and liquid crystal structures has been presented by Brown and Wolken [27], and recent studies by Livolant [28] and by Van Winkle *et al.* [29] reveal that some chromosomes can be considered as strongly elongated cholesteric droplets. Bouligand and Livolant [30] have found numerous biopolymers forming 'Dirac monopole' defects discussed above. One might hope that liquid crystal dispersions would be helpful as the simplest models for deciphering some properties of biological systems; note that the size of biological unit blocks, the cells, is of the order of 1–10 microns. However, the analogy between the liquid crystal dispersions and 'proto-organisms' remains quite remote: a 'proto-organism' should participate in the dissipation of energy; it must be 'semipermeable' to allow the flux of energy and of some selected forms of matter; there should be also some mechanism of division accompanying growth to keep the surface-to-volume ratio relatively low and thus to facilitate the interchange of energy and matter with the surrounding matrix. Although the liquid crystal droplets can possess non-trivial inner structures and a non-spherical shape, they usually preserve their cohesiveness because of the positiveness of the surface-tension coefficient. Quite surprisingly, there is an exception: spontaneous division of chiral liquid crystal droplets has been observed during a specific sequence of phase transitions during temperature *decrease* [31]. This phenomenon illustrates another unusual feature of liquid crystal dispersions that cannot be found in their isotropic counterparts.

Anchoring phenomena at the liquid crystal–isotropic fluid interface *per se* are practically unexplored. Here one might expect orientational analogues of electrocapillarity, i.e. the dependence of the anchoring energy and 'easy orientations' on the concentration of ions or surfactants. Finally, both the confinement and the presence of defects make it necessary to explore the role of the so-called divergence elasticity of liquid crystals.

I thank Prof. S. Lagerwall for the invitation to participate in the Liquid Crystal Symposium held in honour of Prof. G. W. Gray. Useful discussions with P. Crooker, T. C. Lubensky, P. Palffy-Muhoray and E. M. Terentjev helped in the selection of material for this review. I enjoyed collaboration with M. V. Kurik, Yu. A. Nastishin and G. E. Volovik on the topics presented. This work was partially supported by the National Science Foundation under grant DMR89-20147 (STC ALCOM).

References

[1] LEHMANN, O., 1890, *Z. phys. Chem.*, **5**, 427; 1904, *Flüssige Kristalle* (Leipzig: Wilhelm Engelmann), 265 S.

[2] OPARIN, A., 1961, *Life, its Nature, Origin and Development* (New York: Academic Press); OPARIN, A. I., 1968, *Genesis and Evolutionary Development of Life* (New York: Academic Press).

[3] LAUFFER, M., and STANLEY, W., 1938, *J. biol. Chem.*, **123**, 507.

[4] FERGASON, J. L., 1985, *SID Digest*, **16**, 68.

[5] DOANE, J. W., VAZ, N. A., WU, B. G., and ZUMER, S., 1986, *Appl. Phys. Lett.*, **48**, 269.

[6] LAVRENTOVICH, O. D., and TARAKHAN, L. N., 1986, *Zhurn. Tech. Phys.*, **56**, 2071 [*Sov. Phys.—Tech. Phys.*, **31**, 1244]; 1990, *Poverkhnost'*, No. 1, 39.

[7] LAVRENTOVICH, O. D., 1990, DSci thesis, Institute of Physics, Academy of Sciences, Kyiv (unpublished).

[8] WILLIAMS, R. D., 1986, *J. Phys. A: Math. Gen.*, **19**, 3222.

[9] LAVRENTOVICH, O. D., 1986, *Zh. Eksp. Teor. Fiz.*, **91**, 1666 [*Sov. Phys. JETP*, **64**, 984].

[10] TOULOUSE, G., and KLÉMAN, M., 1976, *J. Phys. Lett. (Paris)*, **37**, L-149.

[11] VOLOVIK, G. E., and MINEEV, V. P., 1977, *Sov. Phys. JETP*, **45**, 1186 [*Zh. Eksp. Teor. Fiz.*, **72**, 2256].

[12] DUBROVIN, E. A., NOVIKOV, S. P., and FOMENKO, A. E., 1984, 1985, 1990, *Modern Geometry: Methods and Applications*, Parts I–III (New York: Springer) [*Sovremennaya Geometriya* (Nauka, Moscow, 1979)].

[13] DIRAC, P. A. M., 1931, *Proc. Roy. Soc., London*, **A133**, 60.

[14] SALOMAA, M. M., and VOLOVIK, G. E., 1987, *Rev. Mod. Phys.*, **59**, 533.

[15] BLAHA, S., 1976, *Phys. Rev. Lett.*, **36**, 874.

[16] MERMIN, N. D., 1977, in *Quantum Fluids and Solids*, edited by S. B. Trickey, E. Adams and J. Duffy (New York: Plenum), p. 3.

[17] MERMIN, N. D., 1990, *Boojums All The Way Through* (New York: Cambridge University Press), p. 310.

[18] KURIK, M. V., and LAVRENTOVICH, O. D., 1983, *Sov. Phys. JETP*, **58**, 299 [*Zh. Eksp. Teor. Fiz.*, **85**, 511].

[19] KURIK, M. V., and LAVRENTOVICH, O. D., 1988, *Sov. Phys. Usp.*, **31**, 196 [*Usp. Fiz. Nauk*, **154**, 381].

[20] ROBINSON, C., 1956, *Trans. Faraday Soc.*, **52**, 571; ROBINSON, C., WARD, J. C., and BEEVERS, R. B., 1958, *Discuss. Faraday Soc.*, **25**, 29.

[21] VOLOVIK, G. E., and LAVRENTOVICH, O. D., 1983, *Sov. Phys. JETP*, **58**, 1159 [*Zh. Eksp. Teor. Fiz.*, **85**, 1997].

[22] BRAY, A. J., 1993, *Physica A*, **194**, 41.

[23] TERENTJEV, E. M., 1995, *Europhys. Lett.*, **32**, 607.

[24] POULIN, P., STARK, H., LUBENSKY, T. C., and WEITZ, D. A., 1997, *Science*, **275**, 1770.

[25] NEEDHAM, J., 1935, *Order and Life* (Cambridge: MIT Press), pp. 139–140; 1950, *Biochemistry and Morphogenesis* (London: Cambridge University Press).

[26] GRAY, G. W., 1993, *Liquid Crystals—Molecular Self-Assembly*, British Association for the Advancement of Science, Chemistry Session: Molecular Self-Assembly in Science and Life, Presidential Address, Keele.

[27] BROWN, G. H., and WOLKEN, J. J., 1979, *Liquid Crystals and Biological Structures* (New York: Academic Press).

[28] LIVOLANT, F., 1986, *J. Phys. (Paris)*, **47**, 1605.

[29] VAN WINKLE, D. H., DAVIDSON, M. W., CHEN, W.-X., and RILL, R. L., 1990, *Macromolecules*, **23**, 4140.

[30] BOULIGAND, Y., and LIVOLANT, F., 1984, *J. Phys.*, **45**, 1899.

[31] LAVRENTOVICH, O. D., and NASTISHIN, YU. A., 1984, *JETP Lett.*, **40**, 1015 [*Pis'ma Zh. Eksp. Teor. Fiz.*, **40**, 242]; LAVRENTOVICH, O. D., NASTISHIN, YU. A., KULISHOV, V. I., NARKEVICH, YU. S., TOLOCHKO, A. S., and SHIYANOVSKII, S. V., 1990, *Europhys. Lett.*, **13**, 313.